Materials Chemistry

Cite this: *J. Mater. Chem.*, 2011, **21**, 8332

www.rsc.org/materials

PAPER

High-resolution ^{27}Al MAS NMR spectroscopic studies of the response of spinel aluminates to mechanical action

Vladimir Šepelák,†*[ab] Ingo Bergmann,[c] Sylvio Indris,[a] Armin Feldhoff,[bd] Horst Hahn,[a] Klaus Dieter Becker,[be] Clare P. Grey[fg] and Paul Heitjans[bd]

Received 31st October 2010, Accepted 20th December 2010
DOI: 10.1039/c0jm03721d

The response of the local structure of various types of spinel aluminates, $ZnAl_2O_4$ (normal spinel), $MgAl_2O_4$ (partly inverse spinel), and $Li_{0.5}Al_{2.5}O_4$ (fully inverse spinel), to mechanical action through high-energy milling is investigated by means of ^{27}Al MAS NMR. Due to the ability of this nuclear spectroscopic technique to probe the local environment of Al nuclei, valuable quantitative insight into the mechanically induced changes in the spinel structure, such as the local cation disorder and the deformation of the polyhedron geometry, is obtained. It is revealed that, independent of the ionic configuration in the initial oxides, the mechanical action tends to randomize cations over the two non-equivalent cation sublattices provided by the spinel structure. The response of the spinels to mechanical treatment is found to be accompanied by the formation of a non-uniform core–shell nanostructure consisting of an ordered crystallite surrounded by a structurally disordered interface/surface shell region. Based on the comparative NMR studies of the non-treated and mechanically treated spinels, an attempt is made to separate the surface effects from the bulk effects in spinel nanoparticles. The non-equilibrium cation distribution and the deformed polyhedra are found to be confined to the near-surface layers of spinel nanoparticles with the thickness extending up to about 0.7 nm. The cation inversion parameter of the mechanically treated spinel is compared with that of the non-treated material at non-ambient conditions.

Introduction

The energy needed for the activation of chemical reactions is usually provided by heat, light, or electrical potential. Correspondingly, terms such as thermochemistry, photochemistry, or electrochemistry are generally common in the chemistry literature. A fundamentally different way of initiating or accelerating a chemical reaction is the use of mechanical force (action). It should be noted that the idea of inducing a reaction by exerting mechanical action dates back to the end of ninetieth century, when Carey Lea[1] observed the decomposition of silver and mercuric halides by trituration in a porcelain mortar, although the same compounds are known to melt or sublime undecomposed when heated. These experiments are usually considered the first systematic investigations on the chemical effects of mechanical action.‡ In 1919, Ostwald[2] introduced the term *mechanochemistry* into the literature. Mechanically induced chemistry thus has a long history and it continues to be of high importance.[3] New aspects of this field have emerged from recent developments in the nanosciences. With atomic force and scanning tunnelling microscopy techniques, it is meanwhile possible to manipulate single molecules and to eventually induce chemical reactions.[4]

Among structures susceptible to mechanical forces, complex oxides exhibit a wide range of responses. Especially, oxides with the spinel structure have been considered as a convenient model system for the investigation of mechanically induced processes in ionic systems, because of their structural flexibility providing a wide range of physical and chemical behaviour.[5] Despite their deceptively simple structure (Fig. 1), many spinel oxides, namely,

[a]*Institute of Nanotechnology, Karlsruhe Institute of Technology, Hermann-von-Helmholtz-Platz 1, D-76344 Eggenstein-Leopoldshafen, Germany. E-mail: vladimir.sepelak@kit.edu; Fax: +49-721-60826368; Tel: +49-721-60828929*
[b]*Center for Solid State Chemistry and New Materials, Leibniz University Hannover, Callinstrasse 3-3A, D-30167 Hannover, Germany*
[c]*Volkswagen AG, D-38436 Wolfsburg, Germany*
[d]*Institute of Physical Chemistry and Electrochemistry, Leibniz University Hannover, Callinstrasse 3-3A, D-30167 Hannover, Germany*
[e]*Institute of Physical and Theoretical Chemistry, Braunschweig University of Technology, Hans-Sommer-Strasse 10, D-38106 Braunschweig, Germany*
[f]*Chemistry Department, State University of New York, Stony Brook, New York, 11794-3400, USA*
[g]*Chemistry Department, University of Cambridge, Lensfield Rd, Cambridge, CB2 1EW, UK*
† On leave from the Slovak Academy of Sciences, 04353 Košice, Slovakia.

‡ A more complete list of the papers of Carey Lea was published in: L. Takacs, *Bull. Hist. Chem.*, 2003, **28**, 26; L. Takacs, *J. Mater. Sci.*, 2004, **39**, 4987.

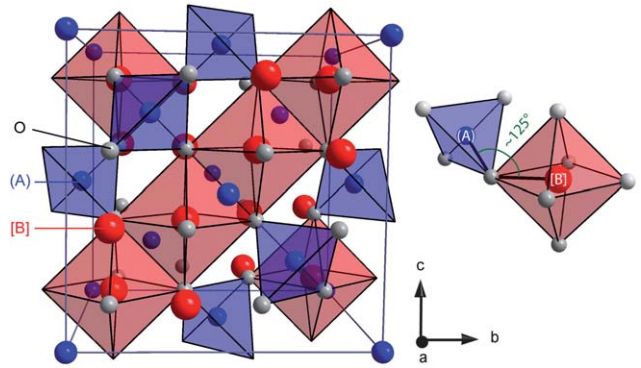

Fig. 1 The cubic unit cell of spinel oxides consists of 56 ions: 32 anions and 24 cations, which are distributed over the sites of tetrahedral (A) and octahedral [B] coordination.

2–3 spinels of the type $M1^{2+}M2_2^{3+}O_4$ and 1–3 spinels $M1_{0.5}^{1+}M2_{2.5}^{3+}O_4$ (where 2–3 and 1–3 refer to the valences of $M1$ and $M2$ cations), exhibit complex disordering phenomena involving the redistribution of cations over the sites of tetrahedral (A) and octahedral [B] coordination provided by the spinel structure.[6] To emphasize the site occupancy at the atomic level, the structural formulas of these materials may be written as $(M1_{1-\lambda}M2_{\lambda})[M1_{\lambda}M2_{2-\lambda}]O_4$ (for 2–3 spinels) and $(M1_{1-\lambda}M2_{\lambda})[M1_{\lambda-0.5}M2_{2.5-\lambda}]O_4$ (for 1–3 spinels), where parentheses and square brackets denote (A) and [B] sites, respectively. The symbol λ represents the so-called degree of inversion defined as the fraction of the (A) sites occupied by trivalent ($M2^{3+}$) cations. For 2–3 spinels, it varies from $\lambda = 0$ (normal spinel) to $\lambda = 1$ (fully inverse spinel), whereas λ takes a value from 0.5 to 1 in the case of 1–3 spinels. The values of $\lambda_s = 2/3$ and $\lambda_s = 5/6$ correspond to the random arrangement of cations in 2–3 and 1–3 spinels, respectively.

It is well recognized that properties of nanooxides prepared by mechanochemical routes are determined to a large extent by the structure of their interfaces/surfaces.[7] Thus, a detailed understanding of such "interface-controlled" materials relies on careful characterization of their local nanostructure. In this article, we will report on the response of the local structure of various types of spinels, $ZnAl_2O_4$ (normal spinel), $MgAl_2O_4$ (partly inverse spinel), and $Li_{0.5}Al_{2.5}O_4$ (fully inverse spinel), to mechanical action through high-energy milling. The important impact of the present work, from the methodology point of view, is the application of ^{27}Al magic angle spinning (MAS) nuclear magnetic resonance (NMR), which makes possible observations on a local atomic scale, and not on a space-averaged scale, as most other experimental techniques do. Thus, for the first time, quantitative information is obtained on the local (short-range) structural disorder induced by mechanical action in the series of related oxides. In addition, based on the comparative MAS NMR studies of the non-treated and mechanically treated spinels, an attempt is made to separate the surface effects from the bulk effects in oxide nanoparticles.

Experimental section

Nanocrystalline spinel aluminates, $ZnAl_2O_4$, $MgAl_2O_4$, and $Li_{0.5}Al_{2.5}O_4$, were produced by high-energy milling of the corresponding bulk oxides (further referred to as the non-treated materials) in a SPEX 8000 shaker mill (Spex CertiPrep Inc., USA) at room temperature. A grinding chamber (50 cm^3 in volume) and a ball (10 mm in diameter) made of zirconia ceramic were used. The ball-to-powder weight ratio was 10 : 1.

The morphology of powders and the sizes of individual crystallites were studied using a combined field-emission (scanning) transmission electron microscope (S)TEM (JEOL JEM-2100F) with a high-resolution pole piece that provides a point resolution better than 0.19 nm at 200 kV. Prior to TEM investigations, powders were crushed in a mortar, dispersed in ethanol, and fixed on a copper-supported carbon grid.

^{27}Al MAS NMR spectra were recorded at room temperature with a Bruker MSL 400 spectrometer at a spinning rate of 15 kHz. The magnetic field was 9.4 T corresponding to a ^{27}Al resonance frequency of 104.2 MHz. A spin-echo pulse sequence was used to acquire the NMR spectra. The repetition time was typically 60 s and chosen that way fully relaxed spectra were obtained. The ^{27}Al chemical shifts are referenced to 1 M $Al(NO_3)_3$ aqueous solution. The degree of inversion, λ, characterizing the distribution of aluminium cations over the (A) and [B] spinel sublattices, was calculated from the intensity ratio of the spectral peaks corresponding to (A)- and [B]-site Al ions, according to formulas $\lambda = 2I_{(A)}/(I_{(A)} + I_{[B]})$ and $\lambda = 2.5I_{(A)}/(I_{(A)} + I_{[B]})$ for 2–3 and 1–3 spinels, respectively.

Results and discussion

During the high-energy milling process, the spinel aluminates are subjected to a continuous fragmentation accompanied by the crystallite size reduction to the nanometer range. The representative high-resolution TEM micrograph of the milled aluminate is shown in Fig. 2. It is revealed that for all the oxides under the present study, the average crystallite size (D) reaches the value of about 10 nm after a prolonged mechanical treatment (1–2 h). It can be seen that the nanostructured oxide possesses the so-called core–shell configuration consisting of structurally ordered regions (often called nanocrystalline grains or crystallites) surrounded by disordered internal interfaces (grain boundaries) and/or external surfaces (near-surface layers). The thickness of the disordered surface shell estimated from the high-resolution TEM is found to vary from 0.2 to 0.4 nm for $MgAl_2O_4$ and $ZnAl_2O_4$, whereas for $Li_{0.5}Al_{2.5}O_4$, it ranges from 0.6 to 0.8 nm (Fig. 2). Recently, the non-uniform core–shell structure of nanoparticles has also been reported for mechanosynthesized ferrites[8] and stannates.[9]

Fig. 3 shows room-temperature ^{27}Al MAS NMR spectra of $ZnAl_2O_4$ milled for various times (t_m). The NMR spectra of $ZnAl_2O_4$, independent of the crystallite size, consist of two well-resolved peaks in the region characteristic of tetrahedrally coordinated aluminium, Al^{3+}(A), (chemical shift $\delta \approx 70$ ppm) and octahedrally coordinated aluminium, Al^{3+}[B], ($\delta \approx 8$ ppm).[10] Note that, in contrast to the (A)-site spectral component, the [B]-site subspectrum exhibits two maxima. This is due to an electric field gradient acting on Al^{3+}[B] nuclei arising from an asymmetric charge distribution around the [B] site (second-order quadrupole interaction).[11] A tiny peak is visible at about 35 ppm corresponding to a small amount of 5-fold coordinated Al.[12]

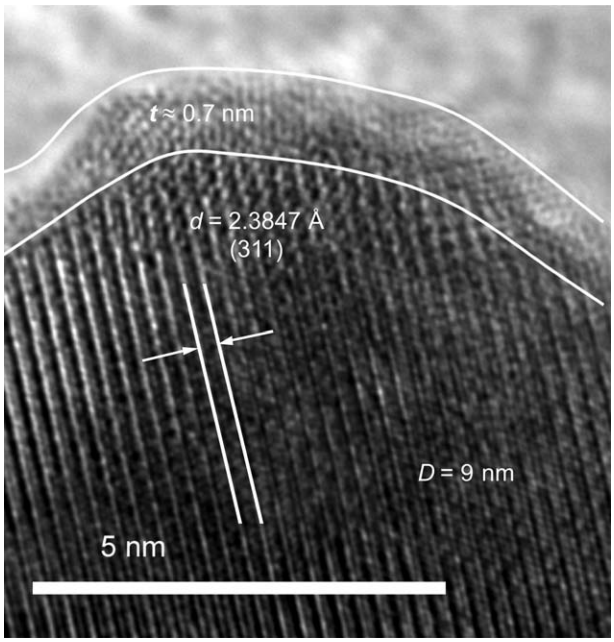

Fig. 2 High-resolution TEM image of the milled $Li_{0.5}Al_{2.5}O_4$. The core–shell configuration of nanoparticles with the thickness of the surface shell of about 0.7 nm is evident. The lattice fringes correspond to the crystallographic plane (311) ($d = 2.3847$ Å) of the $Li_{0.5}Al_{2.5}O_4$ phase (JCPDS PDF 38-1425).

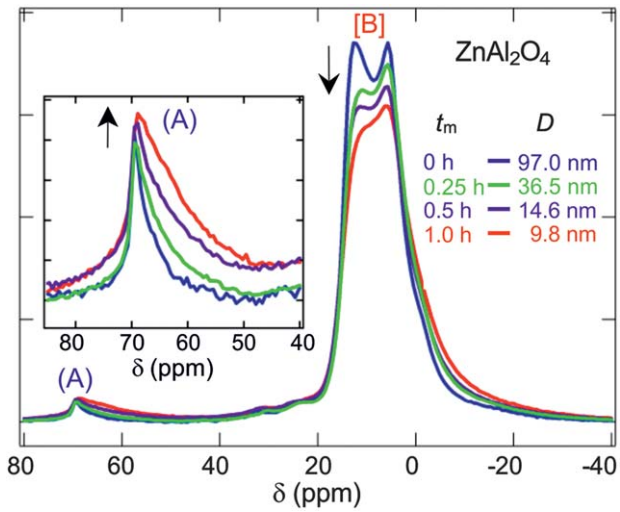

Fig. 3 ^{27}Al MAS NMR spectra of $ZnAl_2O_4$ milled for various times. The milling times (t_m) and the corresponding crystallite sizes (D) are shown in the figure. Arrows emphasize the redistribution of the (A) and [B] spectral intensities. The inset shows the broadening and the increase of the intensity of the (A) subspectrum.

From the intensity ratio of the (A) and [B] spectral components one can easily deduce quantitative information on the cation distribution in the material ($I_{(A)}/I_{[B]} = \lambda/(2 - \lambda)$). The degree of inversion of bulk $ZnAl_2O_4$ ($D = 97(4)$ nm) is found to be $\lambda_c = 0.02(1)$. This indicates that the non-treated $ZnAl_2O_4$ is an almost *normal spinel* with the crystal chemical formula of $(Zn)[Al_2]O_4$. It is clearly visible that mechanical action on $ZnAl_2O_4$ results in the redistribution of the intensities of the (A) and [B] spectral lines, reflecting a decrease of the concentration of Al^{3+} cations on [B] sites and, *vice versa*, an increase of the population of Al^{3+} ions on (A) sites. The important observation is that the degree of inversion of $ZnAl_2O_4$ increases monotonically with decreasing D, reaching the value $\lambda = 0.12(1)$ for crystallites with the size of 9.8(2) nm. Thus, mechanical action on $ZnAl_2O_4$ induces a homogeneous mechanochemical reaction yielding a non-equilibrium cation distribution. The mechanically induced redistribution of Al^{3+} and Zn^{2+} cations between the two non-equivalent spinel lattice sites in $ZnAl_2O_4$ can be quantitatively written as: $(Zn_{0.98}Al_{0.02})[Zn_{0.02}Al_{1.98}]O_4 \rightarrow (Zn_{0.88}Al_{0.12})[Zn_{0.12}Al_{1.88}]O_4$.

The high-resolution ^{27}Al MAS NMR spectra, presented in Fig. 4, show the mechanically induced evolution of the cation disorder in $MgAl_2O_4$. The degree of inversion of the bulk $MgAl_2O_4$ spinel ($D = 150(8)$ nm) is found to be $\lambda_c = 0.23(1)$. This reveals that bulk $MgAl_2O_4$ adopts a *partly inverse spinel* structure of the type $(Mg_{0.77}Al_{0.23})[Mg_{0.23}Al_{1.77}]O_4$. It is clearly visible in Fig. 4 that, similarly as in the case of $ZnAl_2O_4$, mechanical action on $MgAl_2O_4$ is accompanied by an increase of the degree of inversion from $\lambda_c = 0.23(1)$ (for $D = 150(8)$ nm) to $\lambda = 0.31(1)$ for the nanocrystalline ($D = 8.1(3)$ nm) material. This finding is consistent with the recent work on nanostructured $MgAl_2O_4$,[12] where, apart from the non-equilibrium cation distribution on (A) and [B] sites, the presence of additional 5- and 3-fold coordinated cation sites in the near-surface layers of nanoparticles, due to local structural distortion, has been observed. Quantitatively, the mechanically induced process of the cation redistribution in $MgAl_2O_4$ can be formulated as $(Mg_{0.77}Al_{0.23})[Mg_{0.23}Al_{1.77}]O_4 \rightarrow (Mg_{0.69}Al_{0.31})[Mg_{0.31}Al_{1.69}]O_4$.

It is found that mechanochemical processing of $Li_{0.5}Al_{2.5}O_4$ is, contrary to $ZnAl_2O_4$ and $MgAl_2O_4$ spinels, accompanied by a decrease of the concentration of Al^{3+} cations on (A) sites and, consequently, by a decrease of the population of monovalent Li^+ cations on [B] sites. This is clearly demonstrated in the MAS NMR spectra of $Li_{0.5}Al_{2.5}O_4$ milled for various t_m (Fig. 5). It can also be seen that the (A)-site spectral component corresponding to $Li_{0.5}Al_{2.5}O_4$ exhibits two maxima due to an electric field gradient experienced by Al nuclei at (A) sites.[11] Note that this is

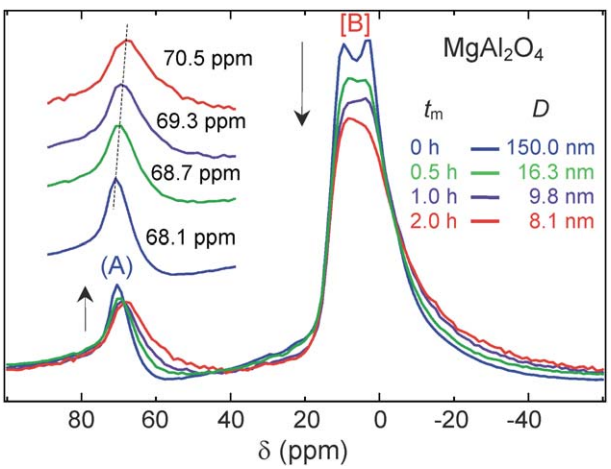

Fig. 4 ^{27}Al MAS NMR spectra of $MgAl_2O_4$ milled for various t_m.

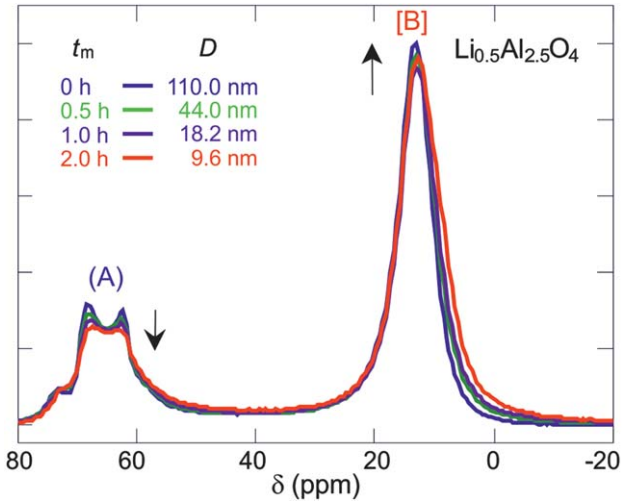

Fig. 5 ^{27}Al MAS NMR spectra of $Li_{0.5}Al_{2.5}O_4$ milled for various t_m.

opposite to the case of $ZnAl_2O_4$ and $MgAl_2O_4$ spinels (compare Fig. 3–5). Moreover, a small shoulder is visible at 73 ppm which does not belong to the second-order quadrupolar lineshape around 65 ppm indicating a minor contribution of a second tetrahedral site. It is revealed that the non-treated $Li_{0.5}Al_{2.5}O_4$ ($D = 110(5)$ nm) adopts a *fully inverse spinel* structure of the type $(Al)[Li_{0.5}Al_{1.5}]O_4$ ($\lambda_c = 1.00(1)$), whereas the degree of inversion of nanosized $Li_{0.5}Al_{2.5}O_4$ with $D = 9.6(4)$ nm is found to be $\lambda = 0.94(1)$. Thus, the crystal chemical formula emphasizing the site occupancy at the atomic level for nanocrystalline lithium aluminate can be written as $(Li_{0.06}Al_{0.94})[Li_{0.44}Al_{1.56}]O_4$. Thus, it can be concluded that mechanical action on spinel aluminates, independent of their ionic configuration in the initial non-treated state, induces a homogeneous mechanochemical reaction which tends to randomize cations among (A) and [B] lattice sites.

An interesting observation is that mechanical action on spinel aluminates brings about both a noticeable broadening and a shift (towards negative chemical shifts) of the (A) and [B] NMR spectral lines (see insets of Fig. 3 and 4), implying a change in the local atomic environments of Al^{3+}(A) and Al^{3+}[B] ions. This variation may be explained by the presence of deformed AlO_6 octahedra and AlO_4 tetrahedra in the nanostructured spinel aluminates.[13] This observation is consistent with the results of previous XRD and Mössbauer investigations of complex oxides,[5,14] where the mechanically induced cation redistribution was found to be accompanied by a deformation of polyhedron geometries.

Taking into account the non-uniform core–shell nanostructure of the milled aluminates (see Fig. 2), the λ values determined by NMR in the present work can be considered as mean values reflecting the cation distribution within the whole volume of spinel nanoparticles, *i.e.*, within their ordered grains and disordered interfaces/surfaces. It was revealed in our work[15] that the major feature of the atomic configuration in the interface/surface regions of spinel oxides prepared by mechanochemical routes is a non-equilibrium ionic distribution characterized by the nearly *random* arrangement of cations. This is in contrast to the ordered grains of nanooxides, which were found to exhibit an equilibrium cation distribution. In other words, considering that grains in the milled $ZnAl_2O_4$, $MgAl_2O_4$, and $Li_{0.5}Al_{2.5}O_4$ possess the same structure as the bulk materials (characterized by the degree of inversion λ_c) and that interfaces/surfaces are structurally disordered due to the random distribution of cations (characterized by $\lambda_s = 2/3$ for 2–3 spinels and $\lambda_s = 5/6$ for 1–3 spinels), the experimentally determined λ values can be expressed as $\lambda = (1 - w)\lambda_c + w\lambda_s$, where w is the volume fraction of interfaces/surfaces. Thus, assuming a spherical shape of the as-prepared $ZnAl_2O_4$ $MgAl_2O_4$, and $Li_{0.5}Al_{2.5}O_4$ nanoparticles, the volume fraction of interfaces/surfaces and their thickness (t) can be estimated using the experimentally determined λ, λ_c and D values.§ It can be seen (Table 1) that the fraction of the structurally disordered interface/surface regions in the spinel nanooxides of comparable crystallite size ($D \approx 10$ nm) ranges from about 16 to 36%. It is interesting to note that the volume fraction of interfaces/surfaces (and consequently their thickness) determined from both HR-TEM and NMR data is about two times larger for $MgAl_2O_4$ and $ZnAl_2O_4$ nanomaterials in comparison with w and t values for nanocrystalline $Li_{0.5}Al_{2.5}O_4$. Assuming that the cation disordering in the surface shell of nanoparticles occurs at the moment of impact by the formation of high-energy localized sites of short lifetime (sometimes called "hot spots" or "thermal spikes"),[3] the different thermal properties such as the melting point, T_m, of the investigated systems (T_m = 2135 °C for $MgAl_2O_4$, T_m = 1950 °C for $ZnAl_2O_4$, T_m = 1290 °C for $Li_{0.5}Al_{2.5}O_4$)[15] can explain this unequal behavior of the aluminates under mechanical treatment. Moreover, various t values observed for the investigated spinels may also be related to their different resistivity to mechanical action (to their different mechanical properties). On average, the volume fraction of interfaces/surfaces in relatively brittle spinel aluminates is found to be smaller than that observed in the mechanochemically prepared spinel ferrites,[8,16,17] which are generally more ductile materials. An interesting observation is that both the non-equilibrium cation distribution and the deformed polyhedra are confined only to the near-surface layers of spinel nanoparticles; the estimated thickness of the interface/surface regions in the nanocrystalline spinel aluminates extends up to about 0.7 nm. We note that, in general, 1 nm is a typical thickness of grain boundary regions in nanostructured mechanosynthesized oxides, such as $MgFe_2O_4$,[16] $NiFe_2O_4$,[17] $MnFe_2O_4$,[18] Ca_2SnO_4,[9] and $CaFe_2O_4$,[8] as well as in $LiNbO_3$,[19] where the grain boundaries were even shown to be amorphous.

Although several mechanisms have been proposed for the cation redistribution processes occurring during high-energy milling of spinels, to the best of our knowledge, no conclusive explanation for the mechanically induced structural disorder in complex oxides has been given yet. For example, Pavlyukhin *et al.*[20] suggested that the non-equilibrium cation distribution in a milled spinel is the result of the shear deformation of the close-packed anion layers in the ⟨111⟩ direction. High local pressures acting on a mechanically treated material may cause a mutual shift of the anion layers in the oxygen sublattice. The investigations dealing with the pressure-induced structural transformations have demonstrated that a spinel at high pressures

§ $w = 100[(\lambda - \lambda_c)/(\lambda_s - \lambda_c)]$; $t = D/2 - [(D/2)^3(100 - w)/100]^{1/3}$.

Table 1 The volume fraction of interfaces/surfaces (w) and their average thickness (t) in nanocrystalline spinel oxides estimated using the experimentally determined mean degree of inversion (λ) and the average crystallite diameter (D). It was taken into account that nanosized crystallites in oxides possess the cation ordered bulk-like structure characterized by the degree of inversion λ_c, whereas the interfaces/surfaces are disordered due to the random distribution of cations (λ_s)

Spinel	D/nm	λ	λ_c	λ_s	w (%)	t/nm
$ZnAl_2O_4$	9.8(2)	0.12(1)	0.02(1)	2/3	15.5(3)	0.3(1)
$MgAl_2O_4$	8.1(3)	0.31(1)	0.23(1)	2/3	18.3(4)	0.3(1)
$Li_{0.5}Al_{2.5}O_4$	9.6(4)	0.94(1)	1.00(1)	5/6	36.0(4)	0.7(1)

exhibits a considerable degree of the cation disorder that can be preserved upon abrupt release of pressure.[21]

There are further attempts to explain the mechanism of the mechanically induced cation disorder in spinels in analogy with the thermally induced inversion occurring at the moment of impact by the formation of high-energy localized sites of short lifetime.[22] Even though we are aware that it is not feasible to formally transfer the processes establishing the equilibrium distribution of cations, taking place during "thermal activation", to the case of mechanical activation, we compare the cation inversion parameter observed in the present case for a milled aluminate with that of the corresponding bulk counterpart at high temperatures. For example, Redfern *et al.*[23] have shown that above 1200 K, the degree of inversion of $MgAl_2O_4$ increases with increasing temperature from about 0.22 to 0.30 at 1662 K. According to these data, the degree of inversion reached in the nanosized milled $MgAl_2O_4$ ($\lambda = 0.31$) corresponds to that of the bulk aluminate at about 1700 K.

To conclude, although in the last few years a surge of investigations in the field of mechanochemistry has resulted in the preparation of nanosized solids by forcing a system to acquire metastable and non-equilibrium configurations, it should be stated that the present mechanochemistry is still in its infancy and is mostly phenomenologically oriented. The elucidation of the microscopic mechanism(s) of the mechanically induced cation redistribution and the determination of the main driving force for mechanochemical processes in complex oxides belong to challenges for fundamental research in the field and require further efforts.

Conclusions

Due to the ability of NMR to discriminate between probe nuclei on the non-equivalent crystallographic sites provided by the spinel structure, valuable insight into the mechanically induced cation redistribution and the deformation of the polyhedron geometry in the spinel aluminates was obtained. It was revealed that mechanical action on the spinels, independent of their ionic configuration in the initial bulk state, randomizes cations among (A) and [B] lattice sites. Thus, for the normal spinel ($ZnAl_2O_4$), the partially inverse spinel ($MgAl_2O_4$) as well as for the fully inverse spinel ($Li_{0.5}Al_{2.5}O_4$), the mechanically induced cation redistribution was found to be directed towards random arrangement ($\lambda_s = 2/3$ for 2–3 spinels; $\lambda_s = 5/6$ for 1–3 spinel). The cation order–disorder process was found to be accompanied by a deformation of polyhedron geometries. Taking into account the non-uniform core–shell structure of spinel nanoparticles, the volume fraction of interfaces/surfaces and their thickness were found to range from about 16 to 36% and from 0.3 to 0.7 nm, respectively. The mechanically treated spinels are in a far-from-equilibrium state with the cation disorder corresponding to that of the bulk counterparts at about 1700 K.

Acknowledgements

The present work was supported by the DFG in the framework of the Priority Program "*Crystalline Nonequilibrium Phases*" (SPP 1415). Partial support by the NSF and the VEGA (2/0174/11) is gratefully acknowledged.

Notes and references

1 M. Carey Lea, *Am. J. Sci.*, 1892, **43**, 527, 3rd Series; M. Carey Lea, *Am. J. Sci.*, 1893, **46**, 241, 3rd Series; M. Carey Lea, *Am. J. Sci.*, 1894, **47**, 377, 3rd Series.
2 W. Ostwald, in *Handbuch der Allgemeinen Chemie, Band 1*, Akademische Verlagsgesellschaft mbH, Leipzig, 1919, p. 70.
3 G. Heinicke, *Tribochemistry*, Akademie Verlag, Berlin, 1984; E. Avvakumov, M. Senna and N. Kosova, *Soft Mechanochemical Synthesis: a Basis for New Chemical Technologies*, Kluwer Academic Publishers, Boston, 2001; K. Tkáčová, *Mechanical Activation of Minerals*, Elsevier, Amsterdam, 1989; V. V. Boldyrev, *Russ. Chem. Rev.*, 2006, **75**, 177; *Mechanochemistry and Mechanical Alloying 2003*, ed. V. Šepelák, K. D. Becker and Z. A. Munir, *J. Mater. Sci.*, 2004, **39**, 4983–5530; S. Kipp, V. Šepelák and K. D. Becker, *Chem. Unserer Zeit*, 2005, **39**, 384; B. Kubias, M. J. G. Fait and R. Schlögl, Mechanochemical Methods, in *Handbook of Heterogeneous Catalysis*, ed. G. Ertl, H. Knözinger, F. Schüth and J. Weitkamp, Wiley-VCH, Weinheim, 2008, vol. 1; F. Delogu and G. Mulas, *Experimental and Theoretical Studies in Modern Mechanochemistry*, Transworld Research Network, Kerala, 2010.
4 A. M. Saitta, P. D. Soper, E. Wasserman and M. L. Klein, *Nature*, 1999, **399**, 46; M. K. Beyer and H. Clausen-Schaumann, *Chem. Rev.*, 2005, **105**, 2921; I. Frank, *Angew. Chem., Int. Ed.*, 2006, **45**, 852; A. Bruckmann, A. Krebs and C. Bolm, *Green Chem.*, 2008, **10**, 1131; C. Weder, *Nature*, 2009, **459**, 45; J. Ribas-Arino, M. Shiga and D. Marx, *Angew. Chem., Int. Ed.*, 2009, **48**, 4190; J. Liang and J. M. Fernández, *ACS Nano*, 2009, **3**, 1628; A. Piermattei, S. Karthikeyan and R. P. Sijbesma, *Nat. Chem.*, 2009, **1**, 133; D. A. Davis, A. Hamilton, J. Yang, L. D. Cremar, D. Van Gough, S. L. Potisek, M. T. Ong, P. V. Braun, T. J. Martínez, S. R. White, J. S. Moore and N. R. Sottos, *Nature*, 2009, **459**, 68; A. N. Sokolov, D.-K. Bučar, J. Baltrusaitis, S. X. Gu and L. R. MacGillivray, *Angew. Chem., Int. Ed.*, 2010, **49**, 4273; I. Park, D. Shirvanyants, A. Nese, K. Matyjaszewski, M. Rubinstein and S. S. Sheiko, *J. Am. Chem. Soc.*, 2010, **132**, 12487; G. Cravotto and P. Cintas, *Angew. Chem., Int. Ed.*, 2010, **49**, 6028; R. Thorwirth, A. Stolle and B. Ondruschka, *Green Chem.*, 2010, **12**, 985; S. Karthikeyan and R. P. Sijbesma, *Nat. Chem.*, 2010, **2**, 436; T. Friščić, *J. Mater. Chem.*, 2010, **20**, 7599.
5 V. Šepelák, I. Bergmann, S. Kipp and K. D. Becker, *Z. Anorg. Allg. Chem.*, 2005, **631**, 993.
6 A. Navrotsky, *Physics and Chemistry of Earth Materials*, Cambridge University Press, Cambridge, 1994.
7 A. Düvel, M. Wilkening, R. Uecker, S. Wegner, V. Šepelák and P. Heitjans, *Phys. Chem. Chem. Phys.*, 2010, **12**, 11251; B. H. Liu, J. Ding, Z. L. Dong, C. B. Boothroyd, J. H. Yin and J. B. Yi, *Phys. Rev. B: Condens. Matter Mater. Phys.*, 2006, **74**, 184427; M. Hofmann, S. J. Campbell, H. Ehrhardt and R. Feyerherm, *J. Mater. Sci.*, 2004, **39**, 5057; V. Pop and I. Chicinas, *J. Optoelectron. Adv. Mater.*, 2007, **9**, 1478; S. Dasgupta, K. B. Kim, J. Ellrich, J. Eckert and I. Manna, *J. Alloys Compd.*, 2006, **424**, 13; V. Šepelák, I. Bergmann, D. Menzel, A. Feldhoff, P. Heitjans, F. J. Litterst and K. D. Becker, *J. Magn. Magn. Mater.*, 2007, **316**, e764; N. Sivakumar, A. Narayanasamy, N. Ponpandian and G. Govindaraj, *J. Appl. Phys.*, 2007, **101**, 084116; E. Manova,

B. Kunev, D. Paneva, I. Mitov, L. Petrov, C. Estournes, C. D'Orleans, J.-L. Rehspringer and M. Kurmoo, *Chem. Mater.*, 2004, **16**, 5689; R. N. Bhowmik, R. Ranganathan, R. Nagarajan, B. Ghosh and S. Kumar, *Phys. Rev. B: Condens. Matter Mater. Phys.*, 2005, **72**, 094405.

8 L. J. Berchmans, M. Myndyk, K. L. Da Silva, A. Feldhoff, J. Šubrt, P. Heitjans, K. D. Becker and V. Šepelák, *J. Alloys Compd.*, 2010, **500**, 68.

9 V. Šepelák, K. D. Becker, I. Bergmann, S. Suzuki, S. Indris, A. Feldhoff, P. Heitjans and C. P. Grey, *Chem. Mater.*, 2009, **21**, 2518.

10 R. L. Millard, R. C. Peterson and B. K. Hunter, *Am. Mineral.*, 1992, **77**, 44.

11 G. Engelhardt and D. Michel, *High Resolution Solid State NMR of Silicates and Zeolites*, John Wiley and Sons, Chichester, 1987.

12 V. Sreeja, T. S. Smitha, D. Nand, T. G. Ajithkumar and P. A. Joy, *J. Phys. Chem. C*, 2008, **112**, 14737.

13 N. Kashii, H. Maekawa and Y. Hinatsu, *J. Am. Ceram. Soc.*, 1999, **82**, 1844; V. Šepelák, S. Indris, I. Bergmann, A. Feldhoff, K. D. Becker and P. Heitjans, *Solid State Ionics*, 2006, **177**, 2487.

14 V. Šepelák, *Ann. Chim.-Sci. Mater.*, 2002, **27**, 61; V. Šepelák, S. Indris, P. Heitjans and K. D. Becker, *J. Alloys Compd.*, 2007, **434–435**, 776.

15 S. M. Olhero, I. Ganesh, P. M. C. Torres and J. M. F. Ferreira, *Langmuir*, 2008, **24**, 9525; R. Hansson, B. Zhao, P. C. Hayes and E. Jak, *Metall. Mater. Trans. B*, 2005, **36**, 187; M. G. Zuev, *Russ. J. Inorg. Chem.*, 2007, **52**, 424.

16 V. Šepelák, A. Feldhoff, P. Heitjans, F. Krumeich, D. Menzel, F. J. Litterst, I. Bergmann and K. D. Becker, *Chem. Mater.*, 2006, **18**, 3057.

17 V. Šepelák, I. Bergmann, A. Feldhoff, P. Heitjans, F. Krumeich, D. Menzel, F. J. Litterst, S. J. Campbell and K. D. Becker, *J. Phys. Chem. C*, 2007, **111**, 5026.

18 M. Muroi, R. Street, P. G. McCormick and J. Amighian, *Phys. Rev. B: Condens. Matter Mater. Phys.*, 2001, **63**, 184414.

19 P. Heitjans, M. Masoud, A. Feldhoff and M. Wilkening, *Faraday Discuss.*, 2007, **134**, 67.

20 Y. T. Pavlyukhin, Y. Y. Medikov and V. V. Boldyrev, *J. Solid State Chem.*, 1984, **53**, 155.

21 R. M. Hazen and A. Navrotsky, *Am. Mineral.*, 1996, **81**, 1021; A. Pavese, G. Artioli and S. Hull, *Am. Mineral.*, 1999, **84**, 905; D. Levy, A. Pavese and M. Hanfland, *Am. Mineral.*, 2003, **88**, 93; S. Da Rocha and P. Thibaudeau, *J. Phys.: Condens. Matter*, 2003, **15**, 7103.

22 A. E. Ermakov, *Fiz. Met. Metalloved.*, 1991, **20**, 5.

23 S. A. T. Redfern, R. J. Harrison, H. St. C. O'Neill and D. R. R. Wood, *Am. Mineral.*, 1999, **84**, 299.